Tubulin-based antimitotic mechanism of E7974, a novel analogue of the marine sponge natural product hemiasterlin

Galina Kuznetsov,[1] Karen TenDyke,[1] Murray J. Towle,[1] Hongsheng Cheng,[1] Junke Liu,[1] Joanne P. Marsh,[1] Shawn E.R. Schiller,[2] Mark R. Spyvee,[2] Hu Yang,[2] Boris M. Seletsky,[2] Christina J. Shaffer,[2] Veronique Marceau,[2] Ye Yao,[2] Edward M. Suh,[2] Silvio Campagna,[3] Francis G. Fang,[3] James J. Kowalczyk,[2] and Bruce A. Littlefield[4]

[1]Divisions of Biology, [2]Discovery Chemistry, [3]Process Chemistry, and [4]Scientific Administration, Eisai Research Institute, Andover, Massachusetts

Abstract

E7974 is a synthetic analogue of the marine sponge natural product hemiasterlin. Here, we show that E7974, such as parental hemiasterlin, acts via a tubulin-based antimitotic mechanism. E7974 inhibits polymerization of purified tubulin *in vitro* with IC_{50} values similar to those of vinblastine. In cultured human cancer cells, E7974 induces G_2-M arrest and marked disruption of mitotic spindle formation characteristic of tubulin-targeted anticancer drugs. Extensive hypodiploid cell populations are seen in E7974-treated cells, indicating initiation of apoptosis after prolonged G_2-M blockage. Consistent with this observation, E7974 induces caspase-3 activation and poly ADP ribose polymerase cleavage, typical biochemical markers of apoptosis. Only a short cellular exposure to E7974 is sufficient to induce maximum mitotic arrest, suggesting that E7974's antitumor effects *in vivo* may persist even after blood levels of the drug decrease after drug administration. Interactions of E7974 with purified tubulin were investigated using two synthetic tritiated photoaffinity analogues incorporating a benzophenone photoaffinity moiety at two different positions of the E7974 scaffold. Both analogues preferentially photolabeled α-tubulin, although minor binding to β-tubulin was also detected. E7974 thus seems to share a unique, predominantly α-tubulin–targeted mechanism with other hemiasterlin-based compounds, suggesting that, unlike many tubulin-targeted natural products and related drugs, the hemiasterlins evolved to mainly target α-tubulin, not β-tubulin subunits. [Mol Cancer Ther 2009;8(10):2852–60]

Received 3/31/09; revised 8/12/09; accepted 8/13/09; published 10/12/09.

The costs of publication of this article were defrayed in part by the payment of page charges. This article must therefore be hereby marked *advertisement* in accordance with 18 U.S.C. Section 1734 solely to indicate this fact.

Note: These data were presented in part at the 96th Annual Meeting of the AACR, Proc Amer Assoc Cancer Res 2005;46: (Abstract 3436).

Current address for B.A. Littlefield: Osher Research Center, Harvard Medical School, Landmark 22A-West, 401 Park Drive, Boston, MA 02215.

Requests for reprints: Galina Kuznetsov, Eisai Research Institute, 4 Corporate Drive, Andover, MA 01810-2441. Phone: 978-837-4854; Fax: 978-794-4910. E-mail: galina_kuznetsov@eri.eisai.com

doi:10.1158/1535-7163.MCT-09-0301

Introduction

The microtubule cytoskeleton plays a critical part in maintaining and regulating cell division (1, 2). Microtubules are polymers comprising α- and β-tubulin heterodimers. During mitosis, microtubules undergo dynamic cycles of lengthening (polymerization) and shortening (depolymerization); these cycles, collectively termed microtubule dynamics, are essential for chromosome attachment to the mitotic spindle and for proper chromosome segregation. Agents that perturb microtubule dynamics by either mechanism are among the most effective anticancer drugs currently in clinical use, and include drugs such as the taxanes and *Vinca* alkaloids (2, 3). Many microtubule-targeting agents currently in use or in clinical trials are natural products or chemically modified, natural product–derived compounds (2).

In this report, we describe the antimitotic mechanism of action of E7974, a novel synthetic analogue of the marine natural product hemiasterlin. Hemiasterlin, a potent cytotoxic tripeptide, was originally isolated from marine sponges (4–6). Hemiasterlin exerts its antiproliferative effects by binding to tubulin, preventing tubulin polymerization, and inducing mitotic arrest (7, 8). However, the *in vivo* anticancer therapeutic efficacy of hemiasterlin is associated with toxicity (5).[5] Thus, we embarked on a medicinal chemistry program to identify hemiasterlin analogues that would be more promising for drug development. In the course of our lead optimization program, we synthesized a large number of analogues of hemiasterlin with variations at every position on the backbone. Optimization of the NH_2-terminal amino acid yielded compounds with high potency against human cancer cells *in vitro*, low susceptibility to PgP-mediated drug efflux, and good pharmaceutical properties. In particular, we found that analogues incorporating cyclic amino acids at the NH_2 terminus, and specifically piperidine-containing amino acids such as pipecolic acid, were very potent. These synthetic efforts culminated in the

[5] Unpublished data.

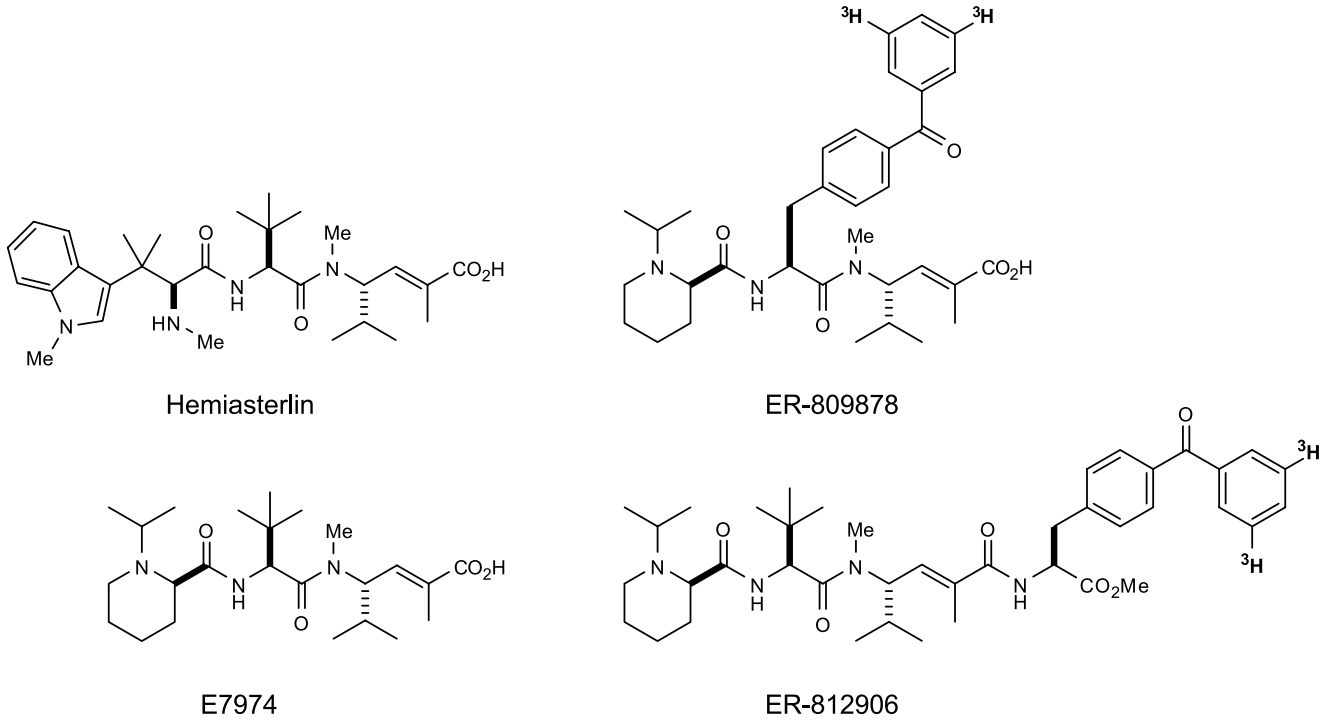

Figure 1. Chemical structures of hemiasterlin, E7974, and photoaffinity probes ER-809878 and ER-812906.

discovery of the N-isopropyl-D-pipecolic acid derivative E7974 (Fig. 1; refs. 9–12). E7974 retains the potent *in vitro* anticancer activity of hemiasterlin,[6] inhibiting the proliferation of a wide variety of human cancer cell types at subnanomolar or low nanomolar concentrations. Importantly, E7974 retains strong potency in cells overexpressing PgP or harboring mutations in the β-tubulin genes that render such cells resistant to the taxanes.[6] E7974 shows strong *in vivo* antitumor efficacy in many human xenograft cancer models, including tumor models that are resistant to paclitaxel.[6] To characterize the anticancer mechanism of E7974, we studied its effects on cell cycle distribution of cultured human cancer cells, formation of mitotic spindles, and induction of apoptosis. Here, we show that E7974 perturbs formation of normal mitotic spindle architecture, blocks cells in the G_2-M phase of the cell cycle after only short exposure times, and induces a long-lasting mitotic blockade that ultimately triggers apoptosis. Based on these favorable preclinical findings, E7974 was selected for human clinical testing, and is currently undergoing phase I clinical trials for cancer (13–16).

Materials and Methods

Materials

E7974 (see, e.g., example 14; ref. 10), and two photoaffinity probes, ER-809878 and ER-812906, were synthesized at Eisai Research Institute (Fig. 1). The photoaffinity moiety chosen was a benzophenone, which was incorporated into two positions on the E7974 scaffold either by replacing the *t*-butylglycine with a *p*-benzoylphenylalanine amino acid (ER-809878) or by attaching a *p*-benzoylphenylalanine amino ester to the COOH terminus of E7974 by an amide bond (ER-812906). The tritium-labeled versions of the probes were synthesized under contract by GE Healthcare (formerly Amersham Biosciences) using appropriate *p*-(3,5-dibromobenzoyl)phenylalanine derivatives prepared at Eisai Research Institute. Vinblastine sulfate was purchased from Sigma-Aldrich.

Cell Culture and E7974 Treatment

U-937 human histiocytic lymphoma cells were obtained from American Type Culture Collection (17) and maintained in suspension culture in RPMI 1640 supplemented with 10% fetal bovine serum, 100 I.U./mL penicillin, 100 μg/mL streptomycin, and 85 mg/mL sodium pyruvate. DU 145 human prostate cancer cells were obtained from American Type Culture Collection and maintained as an adherent culture in Eagle's MEM medium containing 10% fetal bovine serum, 100 I.U./mL penicillin, and 100 μg/mL streptomycin. Stock solutions of E7974 were prepared in 100% anhydrous DMSO (Sigma-Aldrich) and stored in small aliquots at −80 °C until use. Cells were treated with

[6] G. Kuznetsov, K. TenDyke, M.J. Towle, H. Cheng, D. Liu, C. Rowell, J.P. Marsh, J. Wu, S.E.R. Schiller, M.R. Spyvee, H. Yang, B.M. Seletsky, C.J. Shaffer, V. Marceau, Y. Yao, E.M. Suh, S. Campagna, F.G. Fang, J.J. Kowalczyk, B.A. Littlefield. *In vitro* and *in vivo* antitumor activities of a novel hemiasterlin analogue E7974. Manuscript in preparation, and data presented in part at the 96th Annual Meeting of the AACR, Proc Amer Assoc Cancer Res 2005;46: (Abstract 3432).

E7974 for the indicated periods of time following appropriate sterile dilution of DMSO stock solutions into tissue culture medium. Final DMSO concentrations during treatment of cells did not exceed 0.1% (v/v).

Flow Cytometric Analysis of Cell Cycle Distribution

DNA content analysis of U-937 cells was done by flow cytometry as described (18). Briefly, exponentially growing U-937 cells were exposed to 300 nmol/L E7974 for 0 to 24 h. Samples (2–4 × 10^6 cells) were collected by centrifugation, fixed in 70% ethanol/30% saline solution, subjected to RNase digestion, and incubated with 5 μg/mL propidium iodide. Single-channel flow cytometry was done on a Becton Dickinson FACScan flow cytometer. Collection and analysis of data were done using Becton Dickinson CELLQuest software for the Macintosh computer. Doublet events were eliminated from analyses by gating on FL2-W/FL2-A primary plots before histogram analysis of DNA content (measured as FL2-A).

Preparation of Whole Cell Lysates and Immunoblot Analysis

U-937 cells were incubated in the presence or absence of 300 nmol/L E7974 for 24 h. Cells were harvested by centrifugation and lysed in Laemmli's sample buffer [60 mmol/L Tris (pH 6.8), 2% SDS, 10% glycerol, 0.025% bromophenol blue] containing a protease inhibitor cocktail (Calbiochem) consisting of 1 mmol/L AEBSF, 0.8 μmol/L aprotinin, 50 μmol/L bestatin, 15 μmol/L E-64, 20 μmol/L leupeptin hemisulfate, and 10 μmol/L pepstatin A, and supplemented with 1 mmol/L phenylmethylsulfonyl fluoride, 20 μmol/L caspase inhibitor Z-VAD-FMK, and 50 mmol/L DTT. Cell lysates were heated to 100°C for 10 min and subjected to SDS-PAGE. This was followed by Western blot analysis using antibodies against two apoptosis-related protein targets, poly ADP ribose polymerase (PARP), and caspase-3 (BD Pharmingen).

Immunofluorescence Microscopy

DU 145 cells were seeded at 6 × 10^3 cells per chamber in Lab-Tek II 8-chamber #1.5 cover glass slides (Electron Microscopy Sciences). Cells were allowed to adapt to culture during 24 h of incubation at 37 °C without treatment. E7974 and vinblastine were then added to cells at concentrations approximately 3 or 10 times higher than the corresponding IC_{50} values for DU 145 cell growth inhibition.[6] Cells were incubated with the test compounds for 18 h, with control cells receiving equivalent concentrations of DMSO vehicle. After an 18-h incubation period, cells were fixed in 3.7% paraformaldehyde for 10 min and then permeabilized with 0.5% TX-100 solution in PBS for 10 min. Nonspecific protein binding was preblocked by incubation with PBS containing 10% fetal bovine serum. Cells were then incubated with rat monoclonal anti–phosphohistone H3 (Ser28) and/or mouse monoclonal anti–β-tubulin antibodies (Sigma-Aldrich) for 2 h followed by incubation with Alexa Fluor 546–conjugated goat anti-rat IgG and/or Alexa Fluor 488–conjugated goat anti-mouse IgG (Invitrogen Molecular Probes) for 30 min. To visualize DNA, cells were counterstained with 4′,6-diamidino-2-phenylindole

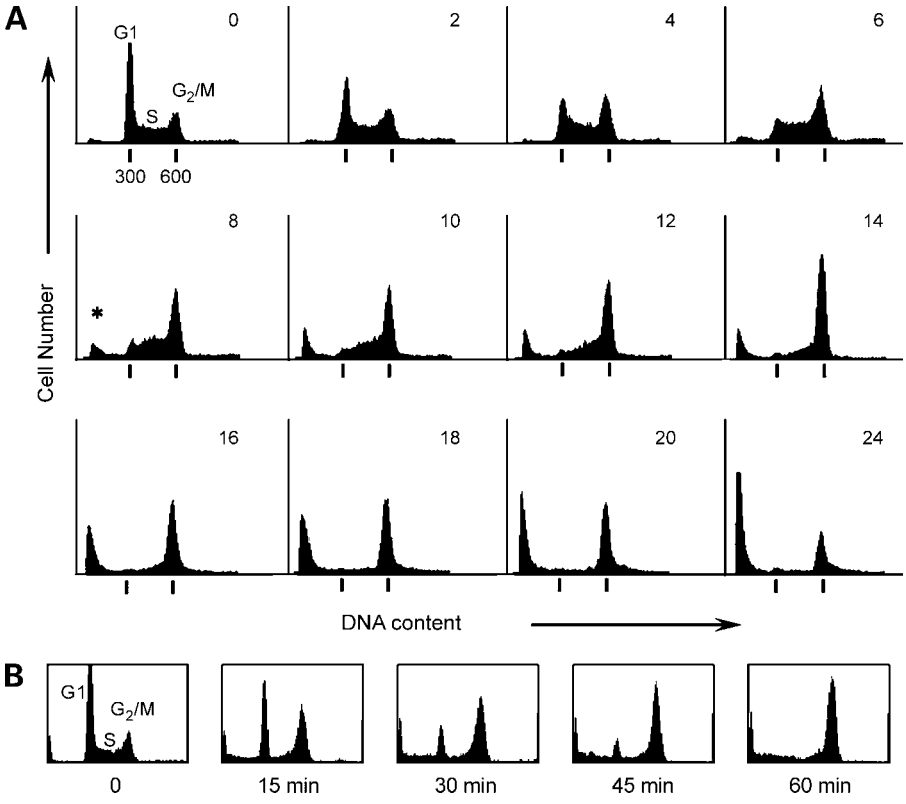

Figure 2. E7974 induces long-lasting G_2-M blocks and appearance of hypodiploid cells in U-937 histiocytic lymphoma cells. Histograms show number of cells per channel (*Y-axis*) versus channel number corresponding to DNA content (*X- axis*). **A,** U-937 cells were treated with 300 nmol/L E7974 for 0 to 24 h, as indicated, followed by staining with propidium iodide and flow cytometric cell cycle analysis as described in Materials and Methods. **B,** U-937 cells were pretreated with 300 nmol/L E7974 for 0 to 60 min at 37°C as indicated. Cells were then harvested by gentle centrifugation, washed in PBS, and resuspended in fresh medium not containing E7974. After 12 h of additional incubation in drug-free medium at 37°C, cells were subjected to flow cytometric cell cycle evaluation as described in Materials and Methods. Percentages of cells in G_2-M as a function of E7974 pretreatment time were as follows: 0 min, 15%; 10 min, 35%; 30 min, 47%; 45 min, 62%; 60 min, 71%.

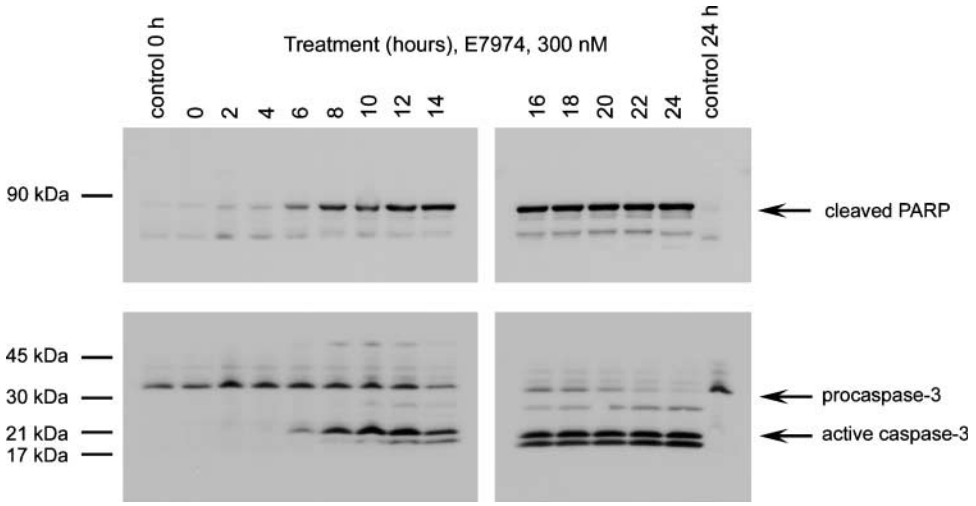

Figure 3. Biochemical evidence of apoptosis induction by E7974. U-937 cells were treated with 300 nmol/L E7974 for 0 to 24 h, followed by Western blot analyses of whole cell lysates using an anti-PARP antibody that recognizes the cleaved (84 kDa) PARP polypeptide (*top*) and an anti–caspase 3 antibody that recognized both uncleaved (32 kDa) and cleaved forms of caspase-3 (*bottom*). Details of all procedures are presented in Materials and Methods.

(DAPI;Invitrogen Molecular Probes). Staining was analyzed using a Leica SP5 confocal microscope under oil immersion.

In vitro Tubulin Polymerization Studies

Tubulin polymerization assays were done using a kit purchased from Cytoskeleton, Inc. following manufacturer's recommended procedure. Briefly, lyophilized bovine brain tubulin was resuspended at 3.2 mg/mL in ice-cold G-PEM buffer [80 mmol/L PIPES (pH 6.9), 2.0 mmol/L $MgCl_2$, 0.5 mmol/L EGTA, 1.0 mmol/L GTP, 5% (v/v) glycerol]. Concentrated (10×) working solutions of test agents were prepared in G-PEM buffer containing 10% DMSO. The final concentration of DMSO in all reactions was 1%. Test agents were placed into wells (10 μL/well) of 96-well half-area plates, which were then prewarmed to 37°C in a VERSAMAX microplate reader (Molecular Devices). Tubulin solution (100 μL/well) was added to wells and mixed with compounds to achieve a final tubulin concentration of 2.9 mg/mL. Plates were returned to the plate reader and read at 340 nm once per minute for 60 min at 37°C using a kinetic protocol. Raw data were processed using the GraphPad Prism program to determine V_{max} and IC_{50} values.

In vitro Tubulin Binding Studies

Bovine brain tubulin was resuspended in G-PEM buffer (described above) at a concentration of 0.5 mg/mL. Tubulin solution (150 μL) was mixed with 3 μL of ^{3}[H]ER-809878 (250 μmol/L, 10 mCi/mL) or 3 μL of ^{3}[H]ER-812906 (333 μmol/L, 10 mCi/mL), respectively. Reaction mixtures were incubated for 30 min at 37°C. Each sample was then distributed into 3 wells (50 μL/well) of a 96-well plate. Plates were placed on ice and exposed to UV light (350 nm) for 90 min using a UV hand lamp (model UVL-28, 8W, UVP) at a distance of 1.5 cm from the sample. Following UV cross-linking, samples were pooled and mixed with Laemmli's sample buffer (Sigma-Aldrich), followed by heating to 100°C for 3 min and SDS-PAGE (7.5% gels). One gel was stained with Coomassie Blue, and a duplicate gel was treated with Amplify reagent (Amersham Biosciences) for 30 min, dried, and exposed to X-ray film for 13 d at −80°C. The film was developed and scanned using a Microtek ScanMaker 6000.

Results

Effect of E7974 on Cell Cycle Distribution

E7974 is a potent inhibitor of cancer cell growth *in vitro* and *in vivo*.[6] To investigate the mechanism of cell growth inhibition, we sought to determine which stage in the cell cycle is interrupted by treatment with E7974. Analysis of cell cycle distribution of U-937 human histiocytic lymphoma cells was done after 0- to 24-hour exposure to E7974. Figure 2A shows the changes in cell cycle distribution as a function of time of exposure to E7974. Exponentially growing U-937 cells were treated with 300 nmol/L E7974 and samples were collected at the times indicated in the top right corner of each panel. Data shown represent relative numbers of cells (*Y*-axis) as a function of fluorescence intensity (*X*-axis). The G_1 and G_2-M DNA contents were adjusted to 300 and 600 arbitrary units, respectively. Untreated cell preparations (0-hour exposure to E7974) show a typical pattern of continuously growing cells distributed in G_1, S, and G_2-M phases (Fig. 2A, *top left*). Treatment with E7974 induced a G_2-M block beginning as early as 4 hours of treatment and increasing continuously thereafter. Concurrently, numbers of cells in G_1 diminished beginning at 4 hours of exposure to E7974. By 10 hours, the G_1 phase had become completely depleted, indicating a complete blockage of new cells progressing through mitosis. An increasing hypodiploid cell population is evident at 8 hours of exposure to E7974 (*), suggesting that cells undergo apoptosis after prolonged blockage in G_2-M (19). After 24 hours of exposure to E7974, nearly all cells were hypodiploid.

To investigate whether induction of apoptosis by E7974 occurs under both anchorage-independent and anchorage-dependent cell culture conditions, we used human prostate cancer DU 145 cells, which grow as a monolayer culture. Effects of E7974 on DU 145 cells were similar to those seen

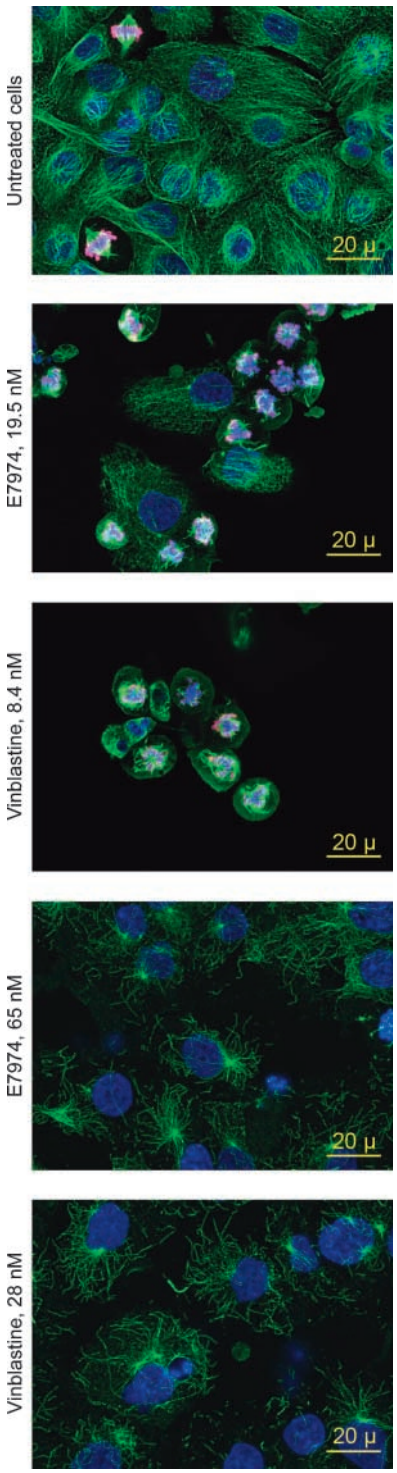

Figure 4. E7974 blocks mitotic spindle formation and decreases microtubule density in DU 145 human prostate cancer cells. *Left,* DU 145 human prostate cancer cells were treated for 18 h: untreated (DMSO), E7974 (19.5 or 65 nmol/L), or vinblastine (8.4 or 28 nmol/L). Cells were then fixed and stained with DAPI (*blue*), anti–β-tubulin (*green*), and anti–phospho-histone H3 (*red*; *top three panels*) or DAPI (*blue*) and anti–β-tubulin (*green*; *two bottom panels*) as described in Materials and Methods. Staining was analyzed using a Leica SP5 confocal microscope at ×400 magnification with oil immersion.

in U-937 suspension cultures: treatment with 300 nmol/L E7974 resulted in G_2-M block and a presence of a significant hypodiploid peak (data not shown). This suggests that DU 145 cells in monolayer culture undergo processes consistent with apoptosis following prolonged E7974-induced mitotic blocks.

In separate experiments, levels of phospho-histone H3 levels, a marker for mitosis (20), were determined by flow cytometry in U-937 and DU 145 cells treated with E7974. Approximately 80% of U-937 cells and 40% of DU 145 cells collected in the G_2-M peak after 14 hours of treatment were positive for phospho-histone H3, suggesting that these fractions of the G_2-M cell populations were actually in mitosis (data not shown). Close to half of the hypodiploid U-937 cells were phospho-histone H3 positive, indicating that the source of hypodiploid cells was directly the mitotic cell population (data not shown). The presence of apoptotic cells in E7974-treated preparations was subsequently confirmed by two biochemical criteria, cleavage of PARP and caspase-3 (see Fig. 3, below).

As described above, continuous exposure to E7974 induced complete mitotic arrest after 10 hours. However, in a clinical setting, drug levels will decline after administration, and cells could potentially recover from effects of the drug and start dividing again. An experiment was thus done to determine the minimal time of exposure to E7974 needed to induce complete mitotic arrest (Fig. 2B). U-937 cells were exposed to 300 nmol/L E7974 for 0 to 60 minutes, the drug was washed away, and the cells were incubated in fresh medium for an additional 12-hour period. Cell cycle distribution was analyzed by flow cytometry at the end of the 12-hour washout period. As shown in Fig. 2B, only a short 60-minute exposure to E7974 was sufficient to induce complete mitotic arrest 12 hours later. By comparison, the half-life of E7974 in patients ranged from 6.3 to 26.9 hours as determined in phase I clinical studies (15). These data suggest that E7974 can induce its maximum effect before the blood levels of the drug decline between drug administrations.

Induction of Apoptosis by E7974

To verify whether the hypodiploid DNA peaks seen in Fig. 2A corresponded to true apoptotic cells, E7974-treated cells were analyzed for the presence of two characteristic biochemical markers of apoptosis, proteolytic cleavage of procaspase-3, and PARP (21–23). Whole cell lysates of U-937 cells treated with E7974 or vehicle were prepared and subjected to SDS-PAGE followed by Western blot analysis with antibodies specific to caspase-3 and PARP. As shown in Fig. 3, procaspase-3 cleavage (activation) and PARP cleavage were both evident after 6 hours of exposure to 300 nmol/L E7974, a similar time at which the appearance of the hypodiploid cell population was detected by flow cytometry (Fig. 2). The presence of apoptotic cells in E7974-treated preparations, suggested by flow cytometry, was therefore confirmed by biochemical criteria.

Similar effects of E7974 (induction of mitotic block and apoptosis) were also observed *in vivo*. In MDA-MB-435 human melanoma xenografts, a single 2.4 mg/kg dose of

E7974 induced a 5- to 6-fold increase in the levels of phospho-histone H3 and cleaved caspase-3 24 h after drug administration (determined by immunohistochemical analysis of tumor tissue).[5]

Disruption of Mitotic Spindle Apparatus in E7974-Treated Cells

The mechanism of E7974-induced cell cycle arrest described above was further studied in DU 145 human prostate cancer cells (Fig. 4). DU 145 cells were treated with 19.5 or 65 nmol/L E7974, and 8.4 or 28 nmol/L vinblastine for 18 h (concentrations that represented ~3 and ~10 times the respective IC_{50} values in DU 145 cells[6]). Treated and untreated cells were stained with anti-tubulin antibodies to visualize microtubules, anti–phospho-histone H3 antibodies to visualize mitotic chromosomes, and with DAPI to label chromosomal material. Stained cells were analyzed by fluorescence microscopy. The untreated cell preparation (*top*) shows only small numbers of cells in mitosis, evident by bright staining with anti–tubulin and anti–phospho-histone H3 antibodies. In the untreated population, the majority of cells were negative for phospho-histone H3, indicating that these cells had not entered mitosis. Two mitotic cells in metaphase can be seen in the untreated cell preparation (*top*) with normal mitotic spindle architecture; nondividing cells show a dense network of microtubules. Treatment with both E7974 and vinblastine induced marked increases in numbers of mitotic cells (positive for phospho-histone H3) as well as disruption of mitotic spindle formation. Most cells in E7974- and vinblastine-treated populations were arrested in mitosis and were unable to complete this process; in these populations, mitotic spindles were highly disorganized tangled arrays of short microtubule fragments, consistent with these two agents being inhibitors of microtubule polymerization. The chromosomal material in E7974-treated preparations was also present in a disorganized fashion, and the chromosomes evidently failed to align at the center of the mitotic cell. All mitotic cells in E7974-treated preparations were positive for phospho-histone H3, indicating that the cells have entered prophase but failed to progress to metaphase; suggesting that the arrest occurred in late prophase or prometaphase. Morphology of the chromosomal material in cells treated with vinblastine

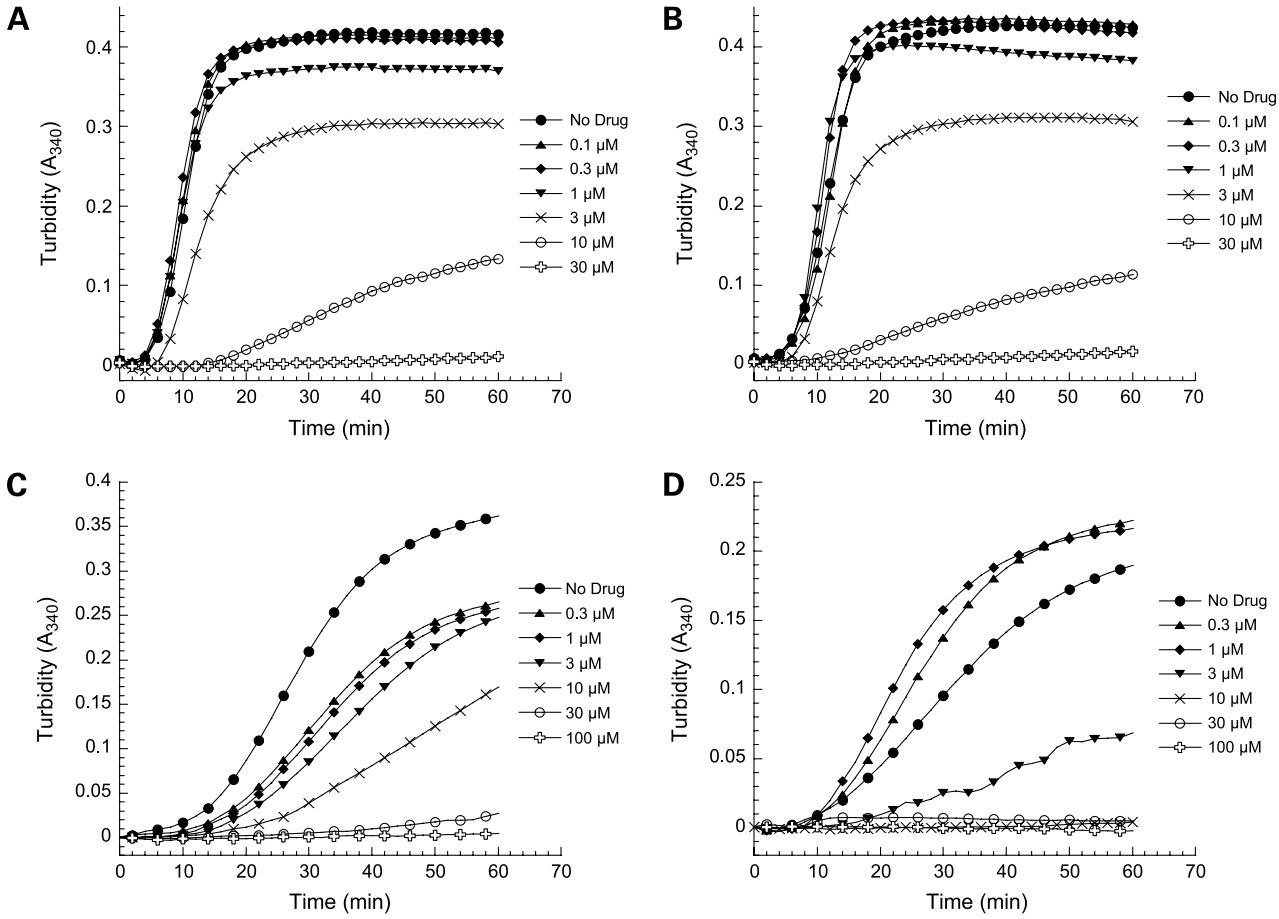

Figure 5. Effects of E7974, vinblastine, and E7974 photoaffinity analogues on tubulin polymerization *in vitro*. The abilities of these compounds to inhibit polymerization of purified bovine brain tubulin *in vitro* was assessed as described in Materials and Methods. Absorbance at 340 nm was determined once per minute for 60 min. *Points,* means of triplicate measurements at each time point. **A,** E7974; **B,** vinblastine; **C,** ER-809878; **D,** ER-812906.

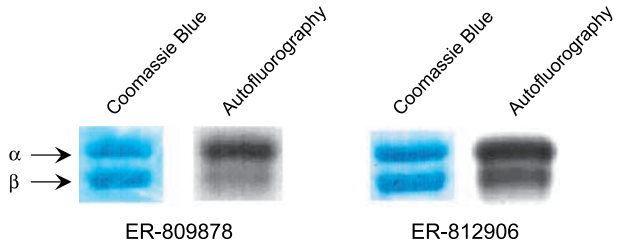

Figure 6. E7974 photoaffinity probes interact dominantly with α-tubulin. Radiolabeled photoaffinity analogues of E7974, [^{3}H]ER-809878, and [^{3}H] ER-812906 were incubated with bovine brain tubulin and UV cross-linked by UV irradiation as described in Materials and Methods. Samples were separated by SDS-PAGE followed by staining with Coomassie blue and processing for autofluorography.

was similar to that of E7974-treated cells. Treatment with higher concentrations of E7974 and vinblastine (19.5 and 8.4 nmol/L, respectively, ~10-fold higher than the respective growth inhibitory IC_{50} values, as shown in the bottom panels) affected microtubules in nonmitotic cells. In these populations, there were marked decreases in microtubule density with both agents. Disruption of normal mitotic spindle formation and decreases in microtubule density are both consistent with E7974's mechanism of action as an inhibitor of tubulin polymerization.

In vitro Inhibition of Tubulin Polymerization by E7974

Effects of E7974 on polymerization of bovine brain tubulin *in vitro* were assessed and compared with those of the known tubulin depolymerizing agent vinblastine. As shown in Fig. 5A and B, both E7974 and vinblastine inhibited tubulin polymerization in a dose-dependent fashion, with E7974 and vinblastine showing similar V_{max} IC_{50} values (3.9 and 3.2 μmol/L, respectively). Thus, E7974 inhibits tubulin polymerization similarly to the known tubulin polymerization inhibitor vinblastine, consistent with observations of G_2-M cell cycle blockage and perturbation of mitotic spindle architecture as described above.

Two Photoaffinity Analogues of E7974 Interact with α-Tubulin

To identify sites of interaction of E7974 with tubulin, two radiolabeled (tritiated) photoaffinity probes were synthesized (Fig. 1). During the course of medicinal chemistry optimization toward the final discovery of E7974, structure-activity relationships had indicated that the scaffold was tolerant to modifications at the t-butylglycine alkyl group and at the COOH terminus (24), at least with regard to cell growth inhibition potency. These two areas of the molecule were therefore chosen for modification into photoaffinity probes (25). The benzophenone moiety was chosen as the photo-labile group; it was incorporated via commercially available *p*-(3,5-dibromobenzoyl)phenylalanine, and the bromine atoms were replaced with tritium under standard hydrogenolysis conditions (or via the analogous nonbrominated p-benzoylphenylalanine derivatives to prepare nontritiated versions of the probes). The rationale for attaching probes both near the NH_2 terminus and at the COOH terminus was that this approach would provide more tubulin binding information than if probe were attached only at either end of the molecule. The benzophenone moiety was incorporated into the E7974 scaffold either by replacing the *t*-butylglycine with a *p*-benzoylphenylalanine amino acid or by attaching a *p*-benzoylphenylalanine methyl ester to the COOH terminus of E7974 by an amide bond (ER-809878 and ER-812906, respectively; Fig. 1C and D). Nonradiolabeled versions of the two probe compounds were prepared and assayed for tubulin polymerization inhibition. Both photoaffinity analogues ER-809878 and ER-812906 inhibited tubulin polymerization *in vitro*, with V_{max} IC_{50} values of 4.8 and 2.2 μmol/L, respectively (Fig. 5C and D). To cross-link the two ^{3}H-photoaffinity analogues to their binding sites on tubulin, probes were incubated with purified bovine brain tubulin and then exposed to UV irradiation. Following binding and cross-linking, α- and β-tubulin subunits were separated by SDS-PAGE and visualized by Coomassie blue and autofluorography (Fig. 6). Identities of the two bands (α- and β-tubulin, upper and lower bands, respectively) were confirmed by Western blot analysis using tubulin type–specific antibodies (data not shown). With ER-809878, binding and cross-linking to α-tubulin (top band) dominated, although faint binding to β-tubulin (lower band) could also be seen. The second probe, ER-812906, also preferentially bound and cross-linked to α-tubulin, although in this case binding to β-tubulin was somewhat greater than with ER-809878. Overall, results with both probes suggest that the E7974 binding site is on α-tubulin but probably very close to the β-tubulin junction within the context of α/β tubulin dimer.

Discussion

Drugs affecting microtubule function, such as the *Vinca* alkaloids and taxanes, are widely used clinically for the treatment of cancer. Despite their widespread use, however, such drugs are not universally efficacious in all cancers, and even when initially useful, their effectiveness is often ultimately limited by development of drug resistance. Thus, considerable opportunities exist for development of improved, microtubule-targeted agents.

Our interest in natural products as drug leads led us to further investigate literature reports regarding the therapeutic promise of hemiasterlin (8). Our initial *in vivo* anticancer evaluation of the natural product was hampered by the strong toxicity of hemiasterlin (5).[5] As a consequence, we initiated a structure-activity study with the intent of identifying a molecule with: (*a*) an acceptable *in vivo* therapeutic window and (*b*) an optimized drug profile and novel therapeutic effects compared with existing antimitotic agents. The first set of analogues synthesized showed that hemiasterlin could be modified and still retain potent antiproliferative and antimitotic activity *in vitro*. This gave us hope that an analogue of hemiasterlin could be found that would possess superior pharmaceutical potential compared with the natural product itself. During the course of efforts to improve *in vivo* anticancer characteristics and pharmaceutical properties of the parent hemiasterlin, we synthesized a

novel N-isopropyl-D-pipecolic acid derivative, E7974. E7974 inhibits proliferation of a wide variety of human cancer cell types, is resistant to PgP-mediated drug efflux, and shows strong anticancer activity against many human cancer xenograft models *in vivo*.[6] The *in vitro* potency of E7974 does not exceed that of parental hemiasterlin, and the favorable characteristic of being resistant to PgP-mediated drug efflux is similar to that of hemiasterlin.[5] However, the major advantage gained by our medicinal chemistry efforts to modify hemiasterlin was in the improved *in vivo* toxicity profile. Although hemiasterlin showed *in vivo* efficacy in several models (5),[5] such efficacy was observed only at doses that were associated with significant toxicity (body weight loss and mortality).[5] In contrast, E7974 shows a much greater efficacy to toxicity ration, inducing strong tumor growth inhibition and tumor regression in several models at or below maximally tolerated doses.[6]

In this report, we describe the antimitotic mechanism of action of E7974. Like parental hemiasterlin, E7974 inhibits polymerization of tubulin with an IC_{50} value similar to that of known tubulin polymerization inhibitor vinblastine. Microtubule dynamics are critical for the proper attachment and segregation of chromosomes during mitosis (1, 2); consistent with this, interference with tubulin polymerization by E7974 results in the inability of cells to complete mitosis. Immunofluorescence analyses of cells treated with E7974 show marked increases in numbers of cells positive for phospho-histone H3, a marker for mitosis, as well as profoundly abnormal mitotic spindle formation. Similar to vinblastine, at low concentrations, E7974 caused marked disruption of normal spindle architecture without noticeable effects on microtubule polymer mass. Decreases in microtubule density was evident with these two agents only at higher concentrations, consistent with reports suggesting that microtubule targeting agents can suppress microtubule dynamics at low concentrations without affecting the microtubule polymer mass (2, 26). These observations are also consistent with the fact that both E7974 and vinblastine are effective inhibitors of cell growth at much lower concentrations than those needed for inhibition of tubulin polymerization *in vitro* (sub to low nanomole per liter versus low micromole per liter, respectively).

Based on other microtubule-targeted drugs, it seems likely that E7974-induced G_2-M arrest followed by apoptosis is related to the observed disruption in mitotic spindle formation. The presence of apoptotic cells in E7974-treated populations was suggested by increases in hypodiploid cells and was further confirmed by marked proteolytic cleavage of caspase-3 and PARP. Other agents that disrupt microtubule dynamics (e.g., taxanes, *Vinca* alkaloids, halichondrins) have also been reported to induce apoptosis following a mitotic arrest (27–31), although the precise signaling pathways triggering apoptosis following mitotic arrest have not been completely elucidated. Recent reports suggest that vinblastine may induce apoptosis by stimulating phosphorylation of Bcl-2 and Bcl-xL (29, 30). Du et al. (29) hypothesized that phosphorylation of these antiapoptotic proteins directly precedes the onset of apoptosis and is carried out by a novel kinase that is activated in response to microtubule damage. Consistent with these findings, we previously reported that exposure of cells to the halichondrin-based microtubule dynamics inhibitor eribulin (previously E7389) leads to Bcl-2 hyperphosphorylation followed by apoptosis (31). Albeit speculative at this point, it is conceivable that Bcl-2 and associated kinase pathways may play a similar role in apoptosis induction by E7974.

Our studies with photoaffinity analogues of E7974 suggest that the agent binds primarily to α-tubulin, which represents an uncommon mechanism of drug interaction with tubulin. We prepared photoaffinity analogues of E7974 with the photo-labile moiety near both ends of the scaffold to probe as widely as possible. The most convenient areas of the scaffold for attaching a benzophenone while maintaining antitubulin activity were at the t-butyl position (ER-809878) and at the COOH terminus (ER-812906). When these molecules were irradiated in the presence of tubulin, it was found that ER-809878 covalently bound dominantly to α-tubulin, whereas ER-812906 bound mainly to α-tubulin but also partially to β-tubulin. Our interpretation of these results is that the E7974 scaffold binds to α-tubulin, near the α/β-tubulin heterodimer interface, such that the COOH terminus of E7974 (or a moiety attached to the COOH terminus) is in proximity to β-tubulin. The benzophenone moiety in the second probe (ER-812906) may have the flexibility and range of motion necessary to extend across the α/β interface.

Most tubulin polymerization inhibitors bind to β-tubulin (2, 32), and thus, polymerization inhibitors that bind to α-tubulin are distinctive. Our results are not inconsistent with those published for two similar photoaffinity analogues of taltobulin (HTI-286), a synthetic analogue of hemiasterlin developed by Wyeth (33, 34). To make its photoaffinity analogues, Wyeth incorporated a benzophenone, respectively, at either the NH_2 terminus or at the *t*-butyl position of taltobulin (34). Thus, although our ER-809878 and one of Wyeth's probes each have a benzophenone moiety in the position of the parent compounds' respective *t*-butyl groups, ER-812906 and Wyeth's other probe have their respective photoaffinity moieties on opposite ends of the respective parent molecules. Unlike our probes, Wyeth's probes were found to label α-tubulin exclusively (34). Although ER-809878 and ER-812906 each have a benzophenone group not present in E7974, it seems likely that the mechanism of E7974's antimitotic action is similar to that of other hemiasterlin analogues (predominant binding to α-tubulin) and is thus distinct from most other classes of tubulin binding agents that principally bind to β-tubulin.

Based on its promising preclinical *in vitro* and *in vivo* efficacy as well as its novel, α-tubulin–targeted mechanism, E7974 was selected for clinical evaluation for cancer, and is currently in phase I clinical trials. Results from those trials will ultimately answer the question of suitability of this agent for cancer therapeutic purposes.

Disclosure of Potential Conflicts of Interest

No potential conflicts of interest were disclosed.

References

1. Desai A, Mitchison TJ. Microtubule polymerization dynamics. Annu Rev Cell Dev Biol 1997;13:83–117.

2. Jordan M, Wilson L. Microtubules as a target for anticancer drugs. Nat Rev Cancer 2004;4:253–65.

3. Giannakakou P, Sackett D, Fojo T. Tubulin/microtubules: still a promising target for new chemotherapeutic agents. J Natl Cancer Inst 2000;92: 182–3.

4. Talpir R, Bemyahu Y, Kashman Y. Hemiasterlin and geodiamolide TA; two new cytotoxic peptides from the marine sponge hemiasterella minor. Tetrahedron Lett 1994;35:4453–6.

5. Coleman JE, de Silva ED, Kong F, Andersen RJ. Cytotoxic peptides from the marine sponge Cymbastela sp. Tetrahedron 1995;51:10653–62.

6. Gamble WR, Durso NA, Fuller RW, et al. Cytotoxic and tubulin-interactive hemiasterlins from Auletta sp. and Siphonochalina spp. sponges. Bioorg Med Chem 1999;7:1611–5.

7. Bai R, Durso N, Sackett DL, Hamel E. Interactions of the sponge-derived antimitotic tripeptide hemiasterlin with tubulin: comparison with dolastatin 10 and cryptophycin. Biochemistry 1999;38:14302–10.

8. Anderson H, Coleman J, Andersen R, Roberge M. Cytotoxic peptides hemiasterlin, hemiasterlin A and hemiasterlin B induce mitotic arrest and abnormal spindle formation. Cancer Chemother Pharmacol 1997;39:223–6.

9. Kowalczyk J, Kuznetsov G, Schiller S, Seletsky B, Spyvee M, Yang H. Hemiasterlin derivatives and uses thereof. US patent 7,064,211 2006.

10. Kowalczyk J, Kuznetsov G, Schiller S, Seletsky B, Spyvee M, Yang H. Hemiasterlin derivatives and uses thereof. US patent 7,192,972 March 20, 2007.

11. Kowalczyk J, Kuznetsov G, Schiller S, Seletsky B, Spyvee M, Yang H. Preparation of hemiasterlin derivatives as antitumor agents. PCT Int Appl. WO-2003082268 A2 20031009 March 22, 2002.

12. Kowalczyk J, Schiller S, Seletsky B, et al. Hemiasterlin derivatives and uses thereof. Int Appl. PCT/US2004/030921, filed September 22, 2004, published as WO 2005/030794 A2 20050407, on April 7, 2005 September 22, 2004.

13. Zojwalla NJ, Takimoto CH, Lucarelli AG, et al. A phase I trial of E7974 administered on days 1, 8, and 15 of a 28-day cycle in patients with solid malignancies. J Clin Oncol 2007;25:Abstract no. 2543.

14. Madajewicz S, Zojwalla NJ, Lucarelli AG, et al. A phase I trial of E7974 administered on days 1 and 15 of a 28-day cycle in patients with solid malignancies. J Clin Oncol (Meeting Abstracts) 2007;25:Abstract no. 2550.

15. Mita AC, Takimoto CH, Zojwalla NJ, et al. A Phase I trial of the hemiasterlin analogue E7974 administered IV to patients with solid malignancies. AACR-NCI-EORTC International Conference 2007. Abstract no. A155.

16. Rocha Lima CS, Rubin EH, Raez LE, et al. A phase I trial of E7974 administered on day 1 of a 21-day cycle in patients with advanced solid tumors. ASCO Gastrointestinal Cancers Symposium 2008. Abstract no. 326.

17. Sundstrom C, Nilsson K. Establishment and characterization of a human histiocytic lymphoma cell line (U-937). Int J Cancer 1976;17: 565–77.

18. Towle M, Salvato K, Budrow J, et al. *In vitro* and *in vivo* anticancer activities of synthetic macrocyclic ketone analogues of halichondrin B. Cancer Res 2001;61:1013–21.

19. Nicoletti I, Migliorati G, Pagliacci M, Grignani F, Riccardi C. A rapid and simple method for measuring thymocyte apoptosis by propidium iodide staining and flow cytometry. Immunol Methods 1991;139:271–9.

20. Goto H, Tomono Y, Ajiro K, et al. Identification of a novel phosphorylation site on histone H3 coupled with mitotic chromosome condensation. J Biol Chem 1999;274:25543–9.

21. Thornberry N, Lazebnik Y. Caspases: enemies within. Science 1998; 281:1312–6.

22. Salvesen G, Dixit V. Caspases: intracellular signaling by proteolysis. Cell 1997;91:443–6.

23. Smulson M, Simbulan-Rosenthal C, Boulares A, et al. Roles of poly (ADP-ribosyl)ation and PARP in apoptosis DNA repair genomic stability and functions of p53 and E2F-1. Adv Enzyme Regul 2000;40:183–215.

24. Kowalczyk J, Schiller S, Spyvee M, et al. Synthetic analogs of the marine natural product hemiasterlin: optimization and discovery of E7974, a novel and potent antitumor agent. Proc Amer Assoc Cancer Res 2005;46:[Abstract 1212].

25. Vodovozova EL. Photoaffinity labeling and its application in structural biology. Biokhimiya (Moscow) 2007;72:5–26.

26. Bhattacharyya B, Panda D, Gupta S, Banerjee M. Anti-mitotic activity of colchicine and the structural basis for its interaction with tubulin. Med Res Rev 2008;28:155–83.

27. Wang L, Liu XM, Kreis W, Budman D. The effect of antimicrotubule agents on signal transduction pathways of apoptosis a review. Cancer Chemother Pharmacol 1999;44:355–61.

28. Srivastava R, Mi Q, Hardwick J, Longo D. Deletion of the loop region of Bcl-2 completely blocks paclitaxel-induced apoptosis. Proc Natl Acad Sci U S A 1999;96:3775–80.

29. Du L, Lyle CS, Chambers TC. Characterization of vinblastine-induced Bcl-xL and Bcl-2 phosphorylation: evidence for a novel protein kinase and a coordinated phosphorylation/dephosphorylation cycle associated with apoptosis induction. Oncogene 2005;24:107–17.

30. Tashiro E, Simizu S, Takada M, Umezawa K, Imoto M. Caspase-3 activation is not responsible for vinblastine-induced Bcl-2 phosphorylation and G2/M arrest in human small cell lung carcinoma Ms-1 cells. Jpn Cancer Res 1998;89:940–6.

31. Kuznetsov G, Towle MJ, Cheng H, et al. Induction of Morphological and biochemical apoptosis following prolonged mitotic blockage by halichondrin B macrocyclic ketone analog E7389. Cancer Res 2004;64: 5760–6.

32. Sengupta S, Thomas SA. Drug target interaction of tubulin-binding drugs in cancer therapy. Expert Rev Anticancer Ther 2006;6:1433–47.

33. Ravi M, Zask A, Rush TS, III. Structure-based identification of the binding site for the hemiasterlin analogue HTI-286 on tubulin. Biochemistry 2005;44:15871–9.

34. Nunes M, Kaplan J, Wooters J, et al. Two photoaffinity analogues of the tripeptide, hemiasterlin, exclusively label α-tubulin. Biochemistry 2005;44:6844–57.